I.P.N. - 91406 ORSAY CEDEX

institut de physique nucléaire CNRS - IN2P3 UNIVERSITÉ PARIS - SUD

10 pages OK

IPNO 93 - 02

"Thermal behaviour analysis of SRF cavities and superconducting HOM couplers : numerical simulation and experimental results"

M. FOUAIDY, T. JUNQUERA (I.P.N. Orsay),

B. AUNE, S. CHEL, J. GRATADOUR, M. JUILLARD, A. MOSNIER (DAPNIA/SEA - CE Saclay),

R. BRIZZI (C.M.A.P.X. - Ecole Polytechnique, Palaiseau).

IPNO 93 - 02

"Thermal behaviour analysis of SRF cavities and superconducting HOM couplers : numerical simulation and experimental results"

M. FOUAIDY, T. JUNQUERA (I.P.N. Orsay),

B. AUNE, S. CHEL, J. GRATADOUR, M. JUILLARD, A. MOSNIER (DAPNIA/SEA - CE Saclay),

R. BRIZZI (C.M.A.P.X. - Ecole Polytechnique, Palaiseau).

Thermal model calculations in superconducting RF cavities

M. FOUAIDY, T. JUNQUERA

Institut de Physique Nucléaire (CNRS - IN2P3) 91406 ORSAY cedex France)

R. BRIZZI

Centre de Mathématiques Appliquées (Ecole Polytechnique - CNRS) 91128 PALAISEAU France

B. AUNE, J. GRATADOUR, M. JUILLARD

DAPNIA/SEA - CE Saclay, 91191 GIF-SUR-YVETTE France

Thermal Model Calculations in Superconducting RF Cavities

M. Fouaidy, T. Junquera
Institut de Physique Nucléaire (CNRS - IN2P3). 91406 ORSAY France
R. Brizzi
Centre de Mathématiques Appliquées (Ecole Polytechnique - CNRS). 91128 PALAISEAU France
B. Aune, J. Gratadour, M. Juillard
DAPNIA / SEA - CE SACLAY. 91191 GIF-SUR-YVETTE France

Abstract

Finite element method based code (using the Modulef library) allows to solve the non-linear heat equation in 2D-axisymmetrical geometries incorporating multiple regions with appropiate boundary and interface conditions. This code can handle such complicated geometries as encountered in Superconducting RF cavities and related cryogenic equipment. Calibrations cells for special surface thermometers developed for SRF cavities operating in superfluid Helium were used to validate this modelling technique. Comparison with the experimental results shows a very good agreement. A modified LHe cooling arrangement of a monocell 1.5 GHz cavity has been studied with this code and the first results are discussed.

1. INTRODUCTION

For future applications of Superconducting Radio-frequency (SRF) cavities, in high energy particle accelerators, these resonators must exhibit accelerating gradients Eacc ≥ 15 MeV/m and unloaded quality factor Qo≥ 5×10^9 at an operating temperature T_{bath} = 1.8 K [1]. To reach these goals an important improvement of the fabrication process and a better understanding of the physical phenomena limiting the cavity performance (Eacc, Qo) are necessary. The thermal behaviour of the cavity is concerned by these limitations and two topics must be considered : a) the general problem of the cavity surface thermal stability when subjected to anomalous RF losses due to local defects or impacting electrons, as well as the effect of the residual surface resistance creating a global heating even in the absence of defects. b) Thermal phenomena related to the cooling conditions of some critical cavity components (main power coupler, high order mode coupler, beam pipes,...). At low temperatures the RF surface resistance, the thermal conductivity, the heat transfer coefficient and the thermal contact resistance are strongly temperature dependent. The steady-state heat equation with the boundary conditions is then strongly non-linear. POISNL, a Finite Element Method (FEM) based computer code can handle such problems with multiple regions (materials) and arbitrarily shaped 2D-axisymmetrical computational domain.

Considering the expensive and large time consuming experimental tests of these devices, the disposal of such tool can greatly improve the design productivity : firstly it can be used to determine the critical parts in the system by numerical simulations and for systematic study of the effect of different parameters, secondly by considering more efficient and simple experimental models in order to validate the design principles.

2 - CODE DESCRIPTION

The POISNL code was developed by R. BRIZZI at the IPN Orsay laboratory for heat transfer analysis in complex geometry devices operating in liquid helium LHe. It was built with the aid of the **MODUL**ar Finite Element Software Library (MODULEF) developed in France by the INRIA [2]and written in Fortran 77.

MODULEF library includes more than 2000 procedures and has a large portability. Among its capabilities : automatic mesh generation (2D and 3D) using different kinds of algorithm, solution of linear systems by direct and iterative methods with dynamic memory allocation, computation of eigen-vectors (eigen-values) of 2D and 3D operators, graphic output modules,... It is now largely used to solve engineering problems in various fields : heat transfer analysis, elasticity, dynamic problems, incompressible fluid flow, electromagnetic fields, resonant cavities ... Briefly, MODULEF consists of modules communicating between them through some invariant data structures. A module is a set of procedures performing one logical process which transforms Input Data Structure into Output Data Structure.

POISNL

The governing equation is the steady-state non-linear heat equation. For a 2D-axisymmetrical computational domain this equation takes the following general form in cylindrical coordinates (r,z) :

$$\frac{1}{r}\frac{\partial\left(r\,k_i(T)\frac{\partial T}{\partial r}\right)}{\partial r}+\frac{\partial\left(k_i(T)\frac{\partial T}{\partial z}\right)}{\partial z}+\sigma_i=0 \qquad (1)$$

where the subscript i concerns parameters inside the i^{th} medium $k_i(T)$ being the material thermal conductivity and σ_i the rate of heat generation per unit volume inside this subdomain. For all the cases discussed in this paper $\sigma_i = 0$.

Typical boundary conditions are : adiabatic wall, prescribed heat flux, heat transfer with LHe (Kapitza conductance H_k) and prescribed temperature.

Using the Garlekin method, the continuous variational formulation of the boundary value problem is derived. The domain discretization is performed by various automatic mesh generators included in the general preprocessor of MODULEF. In our case the finite elements are triangles and Lagrange polynomials of degree 1 are used for interpolation between the triangle nodes. The resulting non-linear system is solved in POISNL by an iterative method using linearisation technique. The linear system is solved by the Cholesky method with dynamic memory

allocation. A relaxation factor is used between two succesive iterations in order to improve the process convergence. The steady-state solution is obtained when the RMS value of the relative variation of the temperature distribution over the whole domain is less than 10^{-5} (typically 20 μK in the considered temperature range).

3 - APPLICATION TO SURFACE THERMOMETRY ON SRF CAVITIES STUDIES

We have developed special thermometers (superfluid "epoxy" thermometers) for accurate temperature measurement of HeII cooled cavity surface. These thermometers are employed as diagnostic probes on SRF cavities in order to detect and locate anomalous RF losses on the cavity surface and electron emission trajectories [3 - 4]. POISNL code was useful for the study of the first test cell, allowing us to analyse the influence of different parameters on the thermometer's thermal response. Moreover, it was possible to simulate and design a new thermometer (superfluid "vacuum" thermometer) with improved efficiency. The results predicted by the numerical model were well confirmed by the experimental data [4].

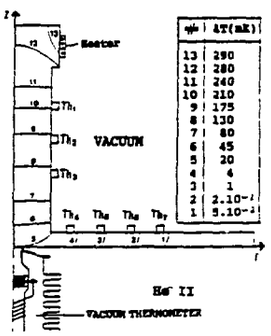

Fig. 1 - Calculated isotherms (POISNL) of the calibration cell for SRF cavity surface thermometry

A new calibration cell was designed consisting of a niobium plate-heater assembly machined from a high purity niobium ingot (RRR = 270). Three resistive thermometers (Th_1 - Th_3) are located on the heater post for in situ thermal conductivity measurements. Four other resistive thermometers(Th_4 - Th_7) are used to measure the radial temperature distribution on the Nb plate heated side. The vacuum thermometer to be calibrated is installed at the center of the He II cooled side of the Nb plate (Fig. 1).The calibration procedure was already discussed [4] so we will focus on the simulation results.

The thermal conductivity $k(T)$ is measured with this cell so the Kapitza conductance H_k at Nb/HeII interface remains the only unknown model parameter of the problem. By using the POISNL code, its value can be adjusted by fitting the experimental temperature distribution to the numerical results. A trial and error method was adopted for this purpose : starting from typical H_k values published in previous works[5 - 6], the temperature field within the niobium specimen is calculated. Then H_k was adjusted by considering the temperature at the vacuum thermometer location and the temperature distribution on the heated side of the niobium specimen and comparing the experimental data with the calculated values and so on until a good fit.

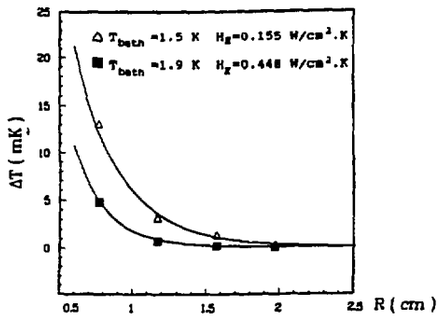

Fig. 2 - Radial temperature distribution on the Nb plate heated side

This method has been used at different bath temperature (1.5 K$\leq T_{bath} \leq$1.9 K) for different heater power (10 mW$\leq Q \leq$ 120 mW). In Fig. 1 are displayed the isotherms calculated by POISNL. In the heater post region the isotherms are horizontal plans giving a high confidence on the $k(T)$ experimental determination. The agreement between experimental and calculated temperature in this region is better than 15 %. The radial temperature distributions ΔT(R) are plotted in Fig. 2 for two different T_{bath} (1.5 K and 1.9 K). Concerning ΔT(R), the difference between experimental and calculated temperatures is less than 0.3 mK which is very close to the measurement resolution (± 0.2 mK).

Finally after H_k adjustement using this method, for different T_{bath}, a least square fit yields the expression :

$$H_k(\mathrm{W/cm^2.K}) = h_o . T_{bath}^{\,n} = 0.0258\, T_{bath}^{\,4.4} \qquad (2)$$

The previous reported data for niobium samples [5 - 6], of different purity and surface treatment shows the following ranges for the h_o and n values : $3.18 \leq n \leq 4.65$ and $0.0072 \leq h_o \leq 0.043$. In conclusion, this adjusting method gives results within the range of the previous experimental data obtained with different measurement techniques [5 - 6].

4 - APPLICATION TO 1.5 GHz SRF SINGLE CELL CAVITY WITH MODIFIED LHe COOLING

In order to simplify the design of cryostats for large electron accelerators, it is planned to surround each cavity with its own LHe vessel. The vessel will not contain the couplers and beam tubes, thus permitting to have all critical connections (RF couplers) inside the insulation vacuum. This should allow an increased safety margin against cavity vacuum leaks. We have checked in the experiment described below, that the behaviour of the cavity at high field level is not affected by the absence of direct LHe cooling of the beam tubes.

A single cell cavity has been modified for this purpose (Fig. 3). Close to one of the iris, the beam tube has been cutted and a niobium disk has been electron beam welded in order to isolate the beam tube from the LHe bath. The beam tube is now located in a separated vacuum chamber closed with stainless steel flanges.

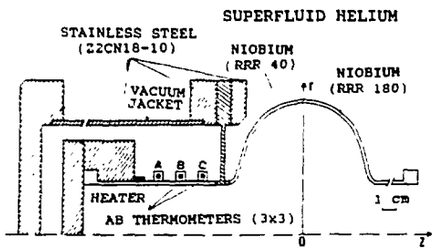

Fig. 3 - 1.5 GHz single cell cavity with modified LHe cooling

A manganin wire heater wrapped around the beam tube and located at z = -11.5 cm from the center of the cavity is used to simulate the coupler RF losses. The resulting temperature gradient along the beam tube is measured by means of nine thermometers located at the periphery of the tube at three different positions A, B, C (z_A = -10.2 cm, z_B = -8.7 cm, z_C = -7.2 cm). At each position 3 thermometers, disposed radially and separated by 120°, measure the mean temperature at this location. The nine thermometers were calibrated in a separate experiment by comparison to two secondary standard thermometers (Germanium and Carbon Glass type) mounted in the same OFHC thermometric copper block. An overall absolute accuracy of ± 10 mK was obtained in the temperature range 1.8 K < T < 16 K.

Using the POISNL code, the special cavity assembly was simulated with the pertinent boundary conditions. The RF power losses q on the cavity surface were introduced by means of an analytical formula deduced by fitting the URMEL code solutions for the magnetic field distribution :

$H(r,z)$ = cte $\quad 0 \leq |z| \leq 3.86$ cm

$H(r,z) \propto exp(-\beta_i z) \quad \beta_1 = 0.95\,\text{cm}^{-1} \quad 3.86 \leq |z| \leq 5.6$

$\beta_2 = 0.61\,\text{cm}^{-1} \quad 5.6 \leq |z| \leq 15.0$

and $q \propto R_S(T)\, H^2$

In all the numerical runs the RF surface resistance $R_S(T)$ includes the BCS term and a residual term R_{res} = 20 nOhm.

The critical part of this special cavity, from the thermal point of view is the joining region between the body of the cavity and the niobium flange welded to the beam tube. This flange acts like a fin "draining" a large part of the heat flux towards LHe bath hence reducing the heat load to the cavity body. A close view of the mesh in this region is presented in Fig. 4.

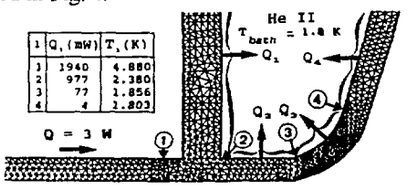

Fig. 4 - Close view of the triangular mesh in the vicinity of the cavity iris - Heat balance in the critical region

In Fig. 5 a typical POISNL result is displayed showing the isotherms in the vicinity of the niobium flange. Notice the isotherms deformation in this region and the effect of HeII cooling on the Nb flange wetted wall. The calculated temperatures at the three different points (A, B, C) were compared to the measured values for different heater power. Concerning the temperature distribution, the discrepancy (≤ 5.5 %) between the two results, which is much larger than the experimental errors, must be attributed to the niobium thermal conductivity curve $k(T)$, which can slightly differ from the niobium effectively used.

Furthermore for an input power Q = 3W, the temperature remains lower than the niobium critical temperature. Moreover the hottest points are located in the region of vanishing surface magnetic field. Using the measured temperature distribution we have calculated the heat flux flowing in the beam tube : the discrepancy between the numerical results and experimental data was less than 24 % in the heater power range 0.5 W ≤ Q ≤ 3W. This error is principally due to uncertainty on $k(T)$.

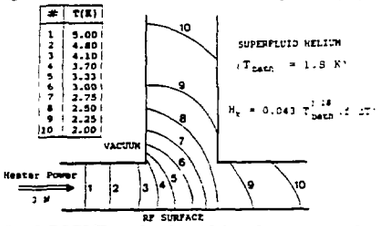

Fig. 5 - POISNL calculated isotherms at the beam tube - Nb flange junction

From the POISNL computed temperature field in the critical region and the H_k value used in the model a heat balance was deduced. The results are summarized in Fig. 4 : for an input power Q = 3W, 1.94 W are drained by the niobium flange towards LHe, the remaining heat flux (1.06 W) is extracted by LHe in the entrance region of the cavity (4.1 cm ≤ |z| ≤ 5.55 cm).

In conclusion $\frac{2}{3}Q$ is drained by the Nb flange and $\frac{1}{3}Q$ is extracted from the cavity body in the region of attenuated RF surface magnetic field ($|z| \geq 3.9$ cm). These results were well confirmed by experimental tests : E_{acc} = 19 MeV/m was reached with $Q_0 \geq 10^{10}$. These values were reproduced up to Q = 3W with just a slight Q_0 decrease at 3W, which was certainly due to the bath temperature increase.

ACKNOWLEDGEMENTS

The authors would like to especially thank J.P. CHARRIER AND F. KOECHLIN from the GECS group (C.E. Saclay) for their participation to some experiments. Sincere thanks are given to the GECS group (I.P.N.Orsay) especially M. ARIANER, A. CARUETTE, N. HAMMOUDI and J C. LE SCORNET for their technical support.

REFERENCES

[1] B. AUNE et al., Proceedings of the 1990 Linear Accelerator Conference - ALBUQUERQUE (USA) 1990.

[2] BERNARDOU, M. et al., "MODULEF : une bibliothèque modulaire d'éléments finis "INRIA (France) 2ème édition 1988.

[3] BRIZZI, R. et al., Proceedings of the ASME Heat Transfer Conference, SEATTLE (USA), june 1990.

[4] FOUAIDY, M. et al., Proceedings of the 5th Workshop on RF Superconductivity, HAMBOURG (Germany), august 1991.

[5] MITTAG, K., Cryogenics 13 (1973) 94.

[6] WILKES, K.E., Ph. D. THESIS, Ohio State Univ. (1978).

Thermal study of HOM couplers for superconducting RF cavities

M. FOUAIDY, T. JUNQUERA

Institut de Physique Nucléaire (CNRS - IN2P3) 91406 ORSAY cedex France

S. CHEL, A. MOSNIER

DSM/DAPNIA/SEA CE - Saclay 91191 GIF-SUR-YVETTE France

Thermal Study of HOM Couplers for Superconducting RF Cavities

M.Fouaidy, T.Junquera
Institut de Physique Nucléaire (CNRS-IN2P3). 91406 ORSAY France

S.Chel, A.Mosnier
DSM/DAPNIA/SEA CE-Saclay 91191 GIF-SUR-YVETTE France

Abstract

The thermal behaviour of a "fish hook" type HOM coupler [1-2] for Superconducting RF Cavities is analyzed by numerical simulation using a 3D finite element based code for both CW (rings, recirculating linacs) and pulsed (s.c. colliders studies like TESLA) accelerator types. Consequently, a thorough study of the thermal stability of this system is necessary in both transient and steady-state regimes. Numerical simulations, assuming anomalous losses at the end of the HOM inner conductor, were performed. The effects of the HOM coupler geometry and the materials thermal conductivity on the critical heat flux inducing the quench of the system are discussed.

I. INTRODUCTION

The superconducting Higher Order Modes (HOM) couplers used for Superconducting Radiofrequency Cavities (SRF) cooled by Liquid Helium (LHe) are generally limited by thermal breakdown induced by various phenomena for accelerating fields E_{acc} in the range 2-5 MeV/m when no efficient cooling of the inner conductor is provided. These E_{acc} values are much smaller than the values to be reached for future projects (e.g. TESLA [3] : E_{acc} = 25 MeV/m). We consider that HOM and beam tubes are located inside the insulation vacuum of the LHe vessel ; this indirect LHe cooling should obviously reduce the thermal quench limit of the HOM couplers. It is then necessary to choose properly the HOM coupler geometry and its construction material in order to increase its capability to whistand anomalous RF losses.

At low temperature, the RF surface resistance, the thermal conductivity (k), the specific heat per unit volum (C_v), the heat transfer coefficient at LHe-metal interfaces are strongly dependent on temperature (T). The resulting heat equation with the pertinent boundary and initial conditions is then nonlinear. Moreover, the system studied is not axisymetrical, hence a 3D computer code is necessary. We used the CASTEM 2000 code [4] for this purpose : this Finite Element Method (FEM) based code can handle such problems in both transient and steady-state conditions for arbitrarly shaped computational domains with multiple regions (i.e. materials).

II. METHOD AND ANALYSIS

A. The boundary value problem

The temperature field T(x,y,z,t), where x,y,z and t are spatial-coordinates and time respectively, within the computational domain Ω is governed by the well-known non-linear 3D Heat Diffusion equation with no heat source :

$$\mathrm{div}\left(k_i(T)\,\nabla T\right) = C_{v_i}\frac{\partial T}{\partial t}$$

where the subscript " i " refers to thermal properties within the region Ω_i.

For the cases of our concern, the typical boundary conditions are : prescribed heat flux q, heat transfer to the LHe at T_{bath} controlled by the Kapitza conductance H_K ($T_{bath} < T_\lambda = 2.176$ K). For this parameter, we have used the following expression [5] :

$$H_K = 0.017\, T_{bath}^{3.62}\left(1 + \frac{3}{2}\left(\frac{\Delta T}{T_{bath}}\right) + \left(\frac{\Delta T}{T_{bath}}\right)^2 + \frac{1}{4}\left(\frac{\Delta T}{T_{bath}}\right)^3\right)$$

where H_K unit is W/cm^2/K, $\Delta T = T - T_{bath}$ and T is the LHe-cooled surface temperature.

Concerning the transient computations, the whole system studied was assumed to be initially at the LHe temperature.

B. Variational problem and approximation

Using the so-called Galerkin Method, the semidiscrete problems corresponding to the above boundary value problem are derived. Briefly, this method constists on subdividing Ω into a set of subvolumes or finite elements, and expanding the solution in terms of FEM using N-components global basis functions. Then, a variational method is applied to these functions leading to N differential (algebraic) equations for time-dependant (steady-state) problems respectively. These equations constitute the semidiscrete variational problem, where the unknown are precisely the nodal values Tj(t) of the temperature field within the Ω-mesh.

C. Resolution Method

In the steady-state case, the above non-linear system is solved by an iterative method using linearisation technique and a relaxation factor for improving the convergence of the process. The steady-state solution is reached when the relative variations of temperature at all the nodes of the Ω-mesh is less than 10^{-3}.

For the transient case, the above equations, discretized in time are solved by a n-step method : the temperature field at a given time is calculated from temperature fields at the n preceeding times (we chose n=2).

Presented at IEEE PAC 93 - Washington D.C. - 17 - 20 May 1993

III. APPLICATION TO THE HOM COUPLER

A. The model and thermal stability criteria

The real system studied (Fig. 1) consists in the beam tube of the cavity, the HOM coupler (diam. : 40 mm and Inner Conductor (IC) diam. : 8 mm), the Nb flange of cryostat tank and the LHe cooled part of the cavity. For numerical simulation, this system was modelled using a slighty modified geometry (Fig. 2) which includes all the parts described previously up to the first iris of the cavity. Notice however that the thermal contact resistances at the sealings (i.e. flanges of the HOM) were neglected, the fish-hook has been replaced by a straight Inner Conductor (IC) which has no influence on the numerical results because the thermal radiations are negligible (T < 10 K), and we have also neglected the heat flux coming from the RF coaxial cable (using a simple Nb cover in place of the upper part of the HOM).

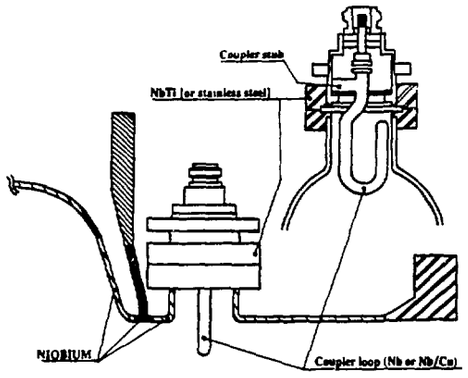

Fig. 1 : Cavity-HOM design.

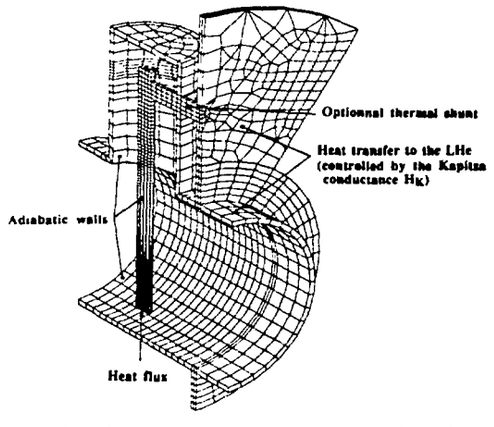

Fig. 2 : Meshed cavity-HOM assembly and applied boundary conditions.

In the defect free case, the total RF losses dissipated on the IC of the HOM remain lower than 0.4 mW (with a peak heat flux density of 40μW/cm^2) for T_{bath} = 2.0 K, E_{acc} = 25 MeV/m and a residual surface resistance R_{res} = 20 nΩ [6]. These very low RF dissipations can not explain an increase of the hot spot temperature beyond the Nb critical temperature Tc = 9.2 K. Consequently, anomalous RF dissipation sources (cavity electron loading, surface defect, multipactor, ...) have to be considered as possible causes of the HOM coupler thermal breakdown. We have then assumed a highly dissipative area, located at the end of the IC, the farest point from the cold source. With this pessimistic assumption we will obtain the minimum heat flux limit Q_c before the quench.

The thermal stability will be insured if two conditions are fulfilled : the temperature T_{max} at the hot spot must be lower than T_c = 9.2 K and the maximum heat flux density transfered to the LHe bath must be below the critical heat flux inducing the Film-Boiling.

B. Steady state regime

The steady-state temperature distribution was computed up to the critical heat flux (Q_c) for the following arrangements and the results are summarized in Table 1. :

1. the whole HOM coupler-cavity assembly is machined from bulk Niobium with RRR = 40, 194 or 570,

2. all these parts are in bulk Niobium (RRR = 40,194 or 570) excepted the IC and the Stub which are made of sputtered Niobium onto a Copper substrate of RRR=300,

3. the same material as in item#1 but with addition of a copper (Cu : RRR=300) thermal shunt between the Coupler and the LHe cryostat flange (see Fig. 2),

4 the same arrangement as in item #2 with addition of the thermal shunt described in item #3.

Nb quality	Arrangement	Critical heat flux Q_c(mW)
RRR 40	# 1	72
RRR 194	# 1	314
RRR 570	# 1	925
RRR 40	# 2	600
RRR 194	# 2	1860
RRR 570	# 2	3418
RRR 40	# 3	79
RRR 194	# 3	347
RRR 570	# 3	1017
RRR 40	# 4	2700*
RRR 194	# 4	3328*
RRR 570	# 4	5430

Table 1 : Critical heat flux inducing the HOM coupler thermal breakdown in the steady-state regime.
* Quench limited by the transition to film boiling on the LHe-cooled Nb flange (heat flux density : 2.4W/cm^2).

Analysing the temperature profiles along the IC for the arrangements #1 and #3 with Q = Q_c,we note that the non-linear effects increase with the Nb RRR, the temperature difference along the IC is around 3.3 K whatever the RRR may be, there is no sensible effect of the thermal shunt on Q_c which increases (from nearly 70 mW to 1 W) with the Nb RRR (see Table 1). The values of the

thermal impedance of the IC ($R_{th} = \Delta T_{IC}/Q_c$) are 46 K/W, 10.5 K/W and 3.6 K/W for RRR = 40, 194 and 570 respectively. So, even in the best arrangement (#3 and Nb RRR = 570), the system is limited by the Niobium thermal conductivity.

In order to overcome this limitation, the arrangement #2 was examined, leading to a reduction by a factor 6 of the IC thermal impedance. The adding of a thermal shunt (arrangement #4) improves greatly Q_c (Fig. 3) due to the sufficiently small thermal impedance (0.6 K/W) of the IC, and in this computation, 70% of Qc is derived through the thermal shunt.

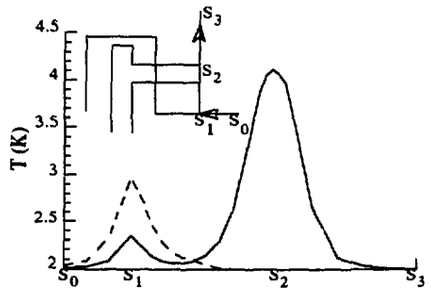

Fig. 3 : Temperature profile along the LHe cooled Nb flange (sketched in the insert).
Full line : with thermal shunt (Q_c = 5.4 W)
Dashed line : without thermal shunt (Q_c = 3.4 W)

C. Transient regime

This study was limited to the arrangement #1 with RRR = 194. The applied heat flux was pulsed close to the TESLA cycle (pulse length τ_p = 2 ms ; f_{rep} = 10 Hz). The maximum hot spot temperature during the RF pulse increases up to 8.6K at the end of the first RF pulse for Q_c=6W, does not recover its initial temperature (i.e. T_{bath}=1.8K) at the end of the first pulse (4.4K), but reaches its stationnary value (9.2K) in nearly 10 pulses (Fig. 4). The higher temperature after an infinity of pulses as function of the heat flux can be evaluated with :

$$T_{max} \cong 3.63\ Q^{0.35} + 0.31\ Q^{0.49}\ .$$

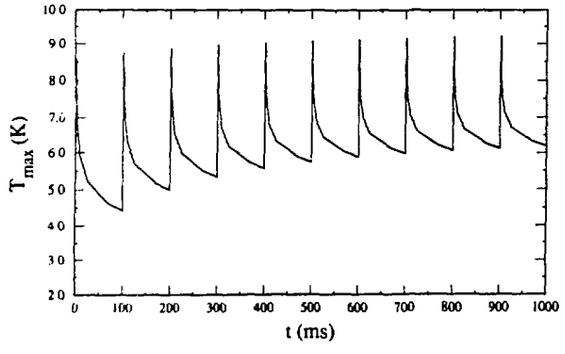

Fig. 4 : Temperature of the hot spot vs time

From the evolution of the temperature along the IC at different times (Fig. 5), the value of 300 cm^2/s is obtained for the diffusion coefficient. Consequently, the perturbation during the RF pulse is localized close to the defect point (diffusion length of 1.5 cm in 2 ms) and the corresponding heat flux can not be evacuated in one complete cycle (110 cm in 100 ms, that is to say, the length of the IC).

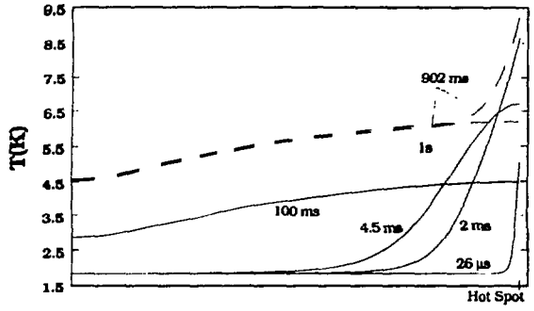

Fig. 5 : Temperature profile along the IC at different times.
Full lines : First pulse
Dashed lines : 10^{th} pulse

IV. CONCLUSION

A HOM coupler heat load capability of over 5 W has been reached in case of a continuous anomalous RF dissipation, by using an IC and a stub made with sputtered Nb onto a Cu substrate, and adding a thermal shunt connected to the LHe flange. In the transient regime, the maximum heat load sustained by the bulk Nb coupler is 6 W. In all the cases and for the corresponding critical heat fluxes, the maximum temperature at the iris of the cavity does not exceed 0.1 K with respect to T_{bath}, so that the thermal stability of the cavity is also insured.

We plane some thermal measurements on a special cavity/HOM assembly, to confirm these calculations and to take into account, if necessary, the effect of the contact resistances at the sealings.

V. REFERENCES

[1] A. Mosnier, "Developments of HOM couplers for superconducting cavities". 4th Workshop on RF Superconductivity, Tsukuba, 1989.

[2] Ph. Bernard and al., "Demountable E/H field HOM for the Nb-sputtered 4-cell LEP cavity". 5th Workshop on RF Superconductivity, Hambourg, 1991.

[3] H. Padamsee, "Review of the superconducting approach to linear colliders". Proc. 3rd Eur. Part. Conf., Berlin, 1992.

[4] P. Verpeaux and al., "A Modern Approch of a Large Computer Code for Structural Analysis", Structural Mechanics Reactor, n° 10, Los Angeles, 1989.

[5] K. Mittag, Cryogenics 13 (1973) 94.

[6] S. Chel, M. Fouaidy, "Thermal behavior of HOM couplers", Internal Report, CE-Saclay/DAPNIA/SEA-93.